

Nonlinear modes in binary bosonic condensates with the pseudo-spin-orbital coupling

D. A. Zezyulin¹, R. Driben^{2,3}, V. V. Konotop¹, and B. A. Malomed²

¹*Centro de Física Teórica e Computacional and Departamento de Física, Faculdade de Ciências, Universidade de Lisboa, Avenida Professor Gama Pinto 2, Lisboa 1649-003, Portugal*

²*Department of Physical Electronics, School of Electrical Engineering, Faculty of Engineering, Tel Aviv University, Tel Aviv 69978, Israel*

³*Department of Physics, University of Paderborn, Warburger Str. 100, D-33098 Paderborn, Germany*

(Dated: August 2, 2018)

We consider a binary Bose-Einstein condensate (BEC) with nonlinear repulsive interactions and linear spin-orbit (SO) and Zeeman-splitting couplings. In the presence of the trapping harmonic-oscillator (HO) potential, we report the existence of even, odd, and asymmetric spatial modes. They feature alternating domains with opposite directions of the pseudo-spin, i.e., anti-ferromagnetic structures, which is explained by the interplay of the linear couplings, HO confinement, and repulsive self-interaction. The number of the domains is determined by the strength of the SO coupling. The modes are constructed analytically in the weakly nonlinear system. The dynamical stability of the modes is investigated by means of the Bogoliubov–de Gennes equations and direct simulations. A notable result is that the multi-domain-wall (DW) structures are stable, alternating between odd and even shapes, while the simplest single-DW structure is *unstable*. Thus, the system features a transition to the *complex ground states* under the action of the SO coupling. The addition of the Zeeman splitting transforms the odd modes into asymmetric ones via spontaneous symmetry breaking. The results suggest possibilities for switching the binary system between states with opposite (pseudo) magnetization by external fields, and realization of similar stable states and dynamical effects in solid-state and nonlinear-optical settings emulated by the SO-coupled BECs.

PACS numbers: 67.85.-d, 03.75.Kk, 03.75.Mn, 05.30.Jp

I. INTRODUCTION

An important application of Bose-Einstein condensates (BECs) is their use for emulating a variety of fundamental effects originating in the realm of condensed-matter physics, in a form which is much easier to handle in atomic gases [1]. Much attention was recently attracted to the implementation of linear couplings between two components of a binary BEC, which emulate the spin-orbit (SO) interactions in solid-state settings, with the respective spinor order parameter mapped into the two-component wave functions of mixtures of different states of the same atomic species [2]. Besides the fundamental interest concerning the dynamics of spinor BECs, the system represents a testbed for the study of artificial gauge fields, which is another topic of a rapidly growing interest [3]. To a great extent, the possibility of emulating condensed-matter effects in ultra-cold gases was brought to the focus of the current research by experiments [4] demonstrating the action of Abelian and non-Abelian synthetic gauge fields in BEC [5].

In addition to simulating condensed-matter phenomena, the studies of SO-coupled BECs reveal new matter-wave effects, produced by the interplay of the SO coupling and the mean-field nonlinearity induced by atomic collisions. Such effects include sophisticated vortical [6] and monopole [7] structures, multi-domain patterns [8], and patterns produced by long-range interactions [9], tricritical points [10], skyrmions [11], solitons [12, 13], interaction with optical lattices [14], etc. Note that the system of coupled Gross-Pitaevskii equations (GPEs) de-

rived in Ref. [12] is tantamount to that describing the co-propagation of two polarizations of light in twisted nonlinear optical fibers [15], hence an additional link between completely different physical settings is the possibility to emulate birefringent optical fibers by the SO-coupled condensates, and *vice versa*. Furthermore, a recent report on the optical implementation of a model simulating massive Dirac fermions [16] indicates the further relevance of results reported below to nonlinear guided-wave optics.

The variety of expected effects in SO-coupled BEC may be greatly enriched when three (or more) atomic levels are employed to define relevant components and interactions between them [3]. In particular, *tripod* atomic schemes give rise to coupled GPEs featuring various nonlinear terms which do not amount to the usual self-phase and cross-phase modulation [17]. Such systems open possibilities for nonlinear control of SO-coupled BECs by means of resonant laser illumination.

While spinor BECs typically give rise to two phases with opposite polarizations of pseudo-spins, and to mixtures of such phases [2, 8, 10], not every form of the SO coupling results in energy splitting between the phases. For such a situation, the role of the nonlinearity is crucially important, as it lifts the degeneracy and induces the phase separation, cf. Ref. [18].

In this work we study nonlinear modes originating from degenerate linear eigenstates in the SO-coupled binary BEC loaded into a harmonic-oscillator (HO) trap, finding a full set of such nonlinear states. We produce basic spatial patterns which exist in the case when the Rashba [19]

and Dresselhaus [20] couplings have equal strengths. The patterns are built of alternating domains with opposite directions of the pseudo-spin, with each state characterized by zero or nonzero total (pseudo-) magnetization. The number of domains is determined by the strength of the SO coupling. The most essential new results concern the stability of the competing states, which is determined by the total magnetization. In contrast to previously studied settings, we demonstrate that the multi-domain-wall (DW) patterns may be *stable* while the single DW is *not*, hence the system's ground state shifts to the complex patterns. We also report a possibility of the dynamical switching between different stable patterns.

II. THE MODEL

We consider the two-component effectively one-dimensional (1D) BEC described by spinor $\Psi = \text{col}\{\psi_1, \psi_2\}$, whose components ψ_1 and ψ_2 represent pseudo-spin components $|\uparrow\rangle$ and $|\downarrow\rangle$. The dynamics of the system is governed by the Hamiltonian, $H = H_0 + H_{\text{int}}$, where, in scaled units, $H_0 = \int_{-\infty}^{+\infty} \Psi^\dagger \mathcal{H} \Psi dx$, $\mathcal{H} = (1/2)(-\partial_x^2 + x^2 + \Omega\sigma_3) + i\kappa\sigma_1\partial_x$, with Pauli matrices $\sigma_{3,1}$, and $x^2/2$ is the axial trapping potential [21]. Zeeman splitting Ω is induced via a constant magnetic field acting along the z -axis, while the SO coupling, accounted by coefficient κ , results from a combined effect of the Rashba and Dresselhaus couplings, and is determined by intensities and wavelengths of laser beams which couple the relevant atomic levels. The interaction terms for the underlying energy-level scheme are represented by $H_{\text{int}} = \int_{-\infty}^{+\infty} [(g_1/2)(|\psi_1|^4 + |\psi_2|^4) + g|\psi_1|^2|\psi_2|^2] dx$ [17]. The derivation of the 1D model from the full 3D one follows the scenario of introducing a tight HO potential of the transverse confinement and factorizing the wave functions into the ground state of that potential and a free longitudinal wave function, which has been elaborated in detail [22]. The structure of the SO-coupled system does not imply any problem in following this scenario, provided that it leads to the usual cubic nonlinearity. The situation may be different for relatively dense BEC, when the resulting 1D model features deviations from the cubic interactions (for the binary condensate without the SO coupling this situation was elaborated in Ref. [23]), which may be a subject for separate analysis [24].

The 1D Hamiltonian gives rise to coupled GPEs,

$$i\partial_t\psi_j = -\frac{1}{2}\partial_x^2\psi_j + \frac{x^2}{2}\psi_j + i\kappa\partial_x\psi_{3-j} - (-1)^j\frac{\Omega}{2}\psi_j + (g_1|\psi_j|^2 + g|\psi_{3-j}|^2)\psi_j, \quad j = 1, 2, \quad (1)$$

which conserve the total number of atoms, $N = N_1 + N_2$, with $N_{1,2} = \int_{-\infty}^{+\infty} |\psi_{1,2}|^2 dx$. Below we consider the generic situation ($g \neq g_1$), and keep N as a free parameter, fixing positive coefficients g_1 and g , which account for the intra- and inter-species repulsive interactions, respectively. Stationary modes of Eq. (1) with chemical

potential μ correspond to $\Psi(x, t) = e^{-i\mu t}\tilde{\Phi}(x)$, where spinor $\tilde{\Phi} = \text{col}\{\phi_1, \phi_2\}$ obeys the system

$$\mu\phi_j = -\frac{1}{2}\phi_j'' + \frac{x^2}{2}\phi_j + i\kappa\phi_{3-j}' - (-1)^j\frac{\Omega}{2}\phi_j + (g_1|\phi_j|^2 + g|\phi_{3-j}|^2)\phi_j, \quad (2)$$

with $\phi_j' \equiv d\phi_j/dx$. In the free space (no trapping potential) and in the absence of the linear coupling, the commonly known condition for the immiscibility of the binary condensate is $g > g_1 > 0$ [26, 27]. The trapping potential and Zeeman splitting shift the transition to the miscibility from $g = g_1$ to larger values of g [28]. Note that, unlike the equations considered in Ref. [12], model (1) is specific to the SO-coupled system, as it did not occur previously in fiber optics. In principle, there is a chance to implement this system in nonlinear optics too, but in a different context, using settings such as the recently reported Dirac model [16], which is obtained from Eq. (2) by neglecting the kinetic-energy terms.

III. ZERO ZEEMAN SPLITTING

At $\Omega = 0$, Eqs. (1) give rise to an evident solution, $\psi_1 = \psi_2 = \exp(i\kappa x + i\kappa^2 t/2)\chi(x, t)$, with function χ obeying the standard GPE: $i\partial_t\chi = [-\frac{1}{2}\partial_x^2 + x^2/2 + (g_1 + g)|\chi|^2]\chi$. Below, we refer to this solution, characterized by nonzero superfluid velocity, as a *current state*. At the same time, the symmetry of system (2) with $\Omega = 0$ admits solutions of two other types: an *odd mode*, with $\phi_2(x) \equiv i\phi_1(-x)$, where $\phi_1(x)$ and $\phi_2(x)$ are purely real and imaginary functions, respectively; and an *even mode*, with $\phi_1(x)$ and $\phi_2(x)$ having opposite parities, e.g., $\phi_1(x)$ is even and real, while $\phi_2(x)$ is odd and imaginary, see examples in Fig. 1. Odd and even modes correspond to symmetric and anti-symmetric distributions of the pseudo-magnetization density, $\mathcal{M} = (|\phi_1(x)|^2 - |\phi_2(x)|^2)/N$, whose integral $M = \int_{-\infty}^{+\infty} \mathcal{M} dx = (N_1 - N_2)/N$ defines the total magnetization.

Possible types of nonlinear modes, which constitute one-parameter families of solutions, can be identified by the analysis of bifurcations of the families from the linear limit, $N \rightarrow 0$ (or, alternatively, $g_1 = g = 0$), which leads to the eigenvalue problem, $\mathcal{H}\tilde{\Phi} = \tilde{\mu}\tilde{\Phi}$ (hereafter, the tilde stands for the linear limit). It is easy to see that the spectrum of this separable system is double-degenerate: $\tilde{\mu}_n = n + (1 - \kappa^2)/2$, $n = 0, 1, 2, \dots$. Eigenvectors, $\tilde{\Phi}_n \equiv \text{col}\{\tilde{\phi}_{1,n}, \tilde{\phi}_{2,n}\}$, can be chosen as arbitrary superpositions of two mutually orthogonal ($\langle \tilde{\Phi}_{n,+}, \tilde{\Phi}_{n,-} \rangle = 0$ [25]) spinors: $\tilde{\Phi}_n = C_+\tilde{\Phi}_{n,+} + C_-\tilde{\Phi}_{n,-}$, where $\tilde{\Phi}_{n,\pm} = e^{\pm i\kappa x} e^{-x^2/2} H_n(x) \text{col}\{1, \pm 1\}$, and $H_n(x)$ is the Hermite polynomial.

However, an arbitrary set of constants C_\pm in $\tilde{\Phi}_n$ does not correspond to nonlinear eigenmodes. To determine the respective constraints, which implies *lifting the degen-*

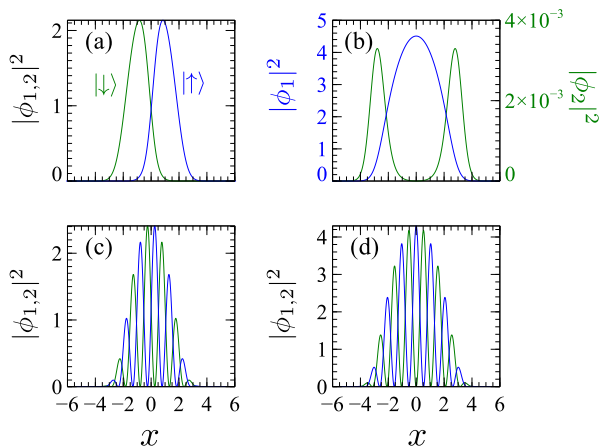


FIG. 1: (Color online) Generic examples of nonlinear modes bifurcating from the lowest linear eigenstate with $n = 0$. Left [right] panels display odd modes for $N = 8$ [even modes with even $\phi_1(x)$ and odd $\phi_2(x)$ for $N = 18$]. Top [bottom] rows correspond to $\kappa = 0.1$ [$\kappa = 3$]. Modes (b)-(d) are stable, while mode (a) is unstable. Other parameters are $g_1 = g/2 = 1$, $\Omega = 0$. Different vertical scales for $\phi_1(x)$ and $\phi_2(x)$ in panel (b) indicate that $|\phi_1(x)| \gg |\phi_2(x)|$.

eracy by the repulsive nonlinearity, we introduce expansions $\mu = \tilde{\mu}_n + \epsilon^2 \mu_n^{(2)} + \dots$ and $\Phi = \epsilon \tilde{\Phi}_n + \epsilon^3 \Phi_n^{(3)} + \dots$, which satisfy Eqs. (2) with $\Omega = 0$ at the leading order with respect to ϵ , which characterizes the strength of the nonlinearity. At order ϵ^3 , one has $(\mathcal{H} - \tilde{\mu}_n)\Phi_n^{(3)} = -\mathbf{F}_n + \mu_n^{(2)}\tilde{\Phi}_n$, with

$$\mathbf{F}_n = \begin{pmatrix} (g_1|\tilde{\phi}_{1,n}|^2 + g|\tilde{\phi}_{2,n}|^2)\tilde{\phi}_{1,n} \\ (g_1|\tilde{\phi}_{2,n}|^2 + g|\tilde{\phi}_{1,n}|^2)\tilde{\phi}_{2,n} \end{pmatrix}. \quad (3)$$

The solvability condition for $\Phi_n^{(3)}$ results in two equations, $\mu_n^{(2)}\langle\tilde{\Phi}_{n,\pm},\tilde{\Phi}_n\rangle = \langle\tilde{\Phi}_{n,\pm},\mathbf{F}_n\rangle$, where constant C_{\pm} are the unknowns. Focusing on the lowest linear eigenstate (the one which corresponds to $n = 0$), it is straightforward to find solutions of the latter equations. One solution has $C_- = 0$ and $C_+ \neq 0$, the respective linear mode being $\tilde{\phi}_{1,n}(x) = \tilde{\phi}_{2,n}(x)$. In the nonlinear regime, it keeps the same structure, $\phi_1(x) \equiv \phi_2(x)$, representing the current state, as defined above. Another solution has $C_+ = \pm iC_-$. In the linear limit, the associated eigenmode is $\tilde{\Phi}_0 = e^{-x^2/2} \text{col}\{\cos(\pi/4 + \kappa x), i\cos(\pi/4 - \kappa x)\}$, which extend into the above-mentioned *odd* nonlinear mode, with $\phi_2(x) \equiv i\phi_1(-x)$. Finally, the third solution, with $C_+ = \pm C_-$ and $\tilde{\Phi}_0 = e^{-x^2/2} \text{col}\{\cos(\kappa x), i\sin(\kappa x)\}$, represents *even* modes in the nonlinear regime. Importantly, *no other solutions* exists in the weakly nonlinear system.

Thus we have identified three families of nonlinear modes bifurcating from the lowest eigenstate $n = 0$. Numerically found examples of the nonlinear modes from these families are shown in Fig. 1. While, as said above, one should expect the immiscibility due to the repulsive interactions, most modes feature the striped antiferro-

magnetic structure, represented by alternating domains of states $|\uparrow\rangle$ and $|\downarrow\rangle$, rather than two large domains separated by a single (DW, which is the case in the conventional binary BEC [28, 29]). It is seen that the number of the domains increases with the SO coupling strength, the single DW being present only in panel 1(a). This patterning is precisely explained by the spatially periodic factors in the above analytical solutions. In qualitative terms, the interplay of the HO trap with the SO coupling gives rise to scale $l \sim 1/\kappa$ that determines the periodicity of the striped patterns in Fig. 1 (the analytical solutions yield $l = \pi/\kappa$). It is relevant to mention that multi-domain patterns were also reported in Ref. [30] in the spinor (three-component) BEC under the action of external magnetic field (without the SO coupling). An essential difference of our system is that the transition between different numbers of domains is controlled by the intrinsic strength of the SO coupling, rather than by an additionally introduced magnetic field. For the SO-coupled system with spin 2, two-dimensional multi-domain patterns were reported in Ref. [31], but the stability of those patterns (which is the main subject of the present analysis) was not studied.

A similar analysis has been performed for higher-order nonlinear modes, i.e. for ones stemming from excited states of the linear system ($n \geq 1$, see above). They also feature the multi-DW structure of the odd and even types, with the number of domains increasing with the strength of the SO coupling, see the examples displayed in Fig. 2.

In view of the coexistence of many multi-DW patterns, their stability is a crucial issue. Here we are meaning the experimentally relevant dynamical stability, determined by the Bogoliubov-de Gennes (BdG) equations derived from Eqs. (1), rather than the thermodynamic stability. The spectrum of the BdG equations was found by means of standard methods for the solution of the corresponding eigenvalue problem [27], and the results were verified by direct simulations of the perturbed evolution of the modes. A surprising conclusion is that the simplest pattern with the single DW, shown in Fig. 1(a), is *unstable*, on the contrary to the situation in the ordinary binary BEC [28, 29], while the multi-DW patterns, displayed in panels (b-d), are *stable*. This finding may be explained by the fact that stable are those structures which comply with the above-mentioned spatial scale l naturally selected by the system. In direct simulations of the perturbed evolution, see Fig. 3), the unstable single-DW state spontaneously develops strong oscillations, in agreement with the oscillatory instability predicted by the BdG analysis. The resulting formation of robust dynamical modes in the form of breathers is a physically relevant result too.

Furthermore, we have found that higher-order nonlinear modes, with the number of domains increasing with strength of the SO coupling, which bifurcate from the excited linear states, with $\mu = \tilde{\mu}_{1,2,\dots}$ (see above), may also be stable in the nonlinear system, see examples of

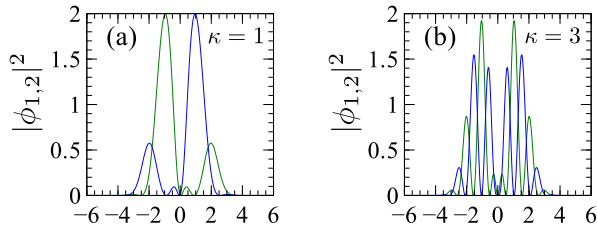


FIG. 2: (Color online) Examples of stable nonlinear modes bifurcating from the first excited ($n = 1$) linear eigenstate (rather than from the ground state with $n = 0$, cf. Fig. 1. Panels (a) and (b) show, severally, odd and even modes for $g_1 = g/2 = 1$ and $\Omega = 0$.

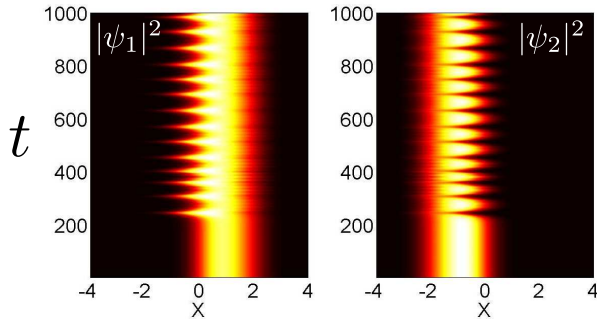


FIG. 3: (Color online) The evolution of the unstable nonlinear mode shown in Fig. 1 (a). Under the action of the instability, the mode spontaneously transforms into a persistent oscillatory state.

stable higher-order modes in Fig. 2.

The full stability chart for the odd and even nonlinear modes originating from $\mu = \tilde{\mu}_0$ is fairly complex, as shown in Fig. 4. For sufficiently small values of κ and in the linear limit $N \rightarrow 0$ only the even modes are stable. This is readily explained by the fact that, at small κ , the system admits an obvious even configuration with almost all atoms falling into a single state, see Fig. 1(b). For larger κ , the stability diagram features a zebra-like structure, with alternating stability regions of the even and odd modes (while the aforementioned current states are completely unstable, cf. Ref. [32]). The stability areas for the odd and even modes approximately (but not precisely) complement each other, which is a consequence of the competition between coexisting nonlinear modes

These stability results are the most essential findings reported in this work, as they demonstrate the previously unreported transition to *complex ground states* in the system, under the action of the SO coupling. In fact, this transition may be expected in diverse systems beyond the model of the linearly-coupled binary BEC.

The stable patterns are naturally characterized by the total pseudo-magnetization M ($M = \pm 1$ means that the condensate is in a single-domain state), and by the mis-

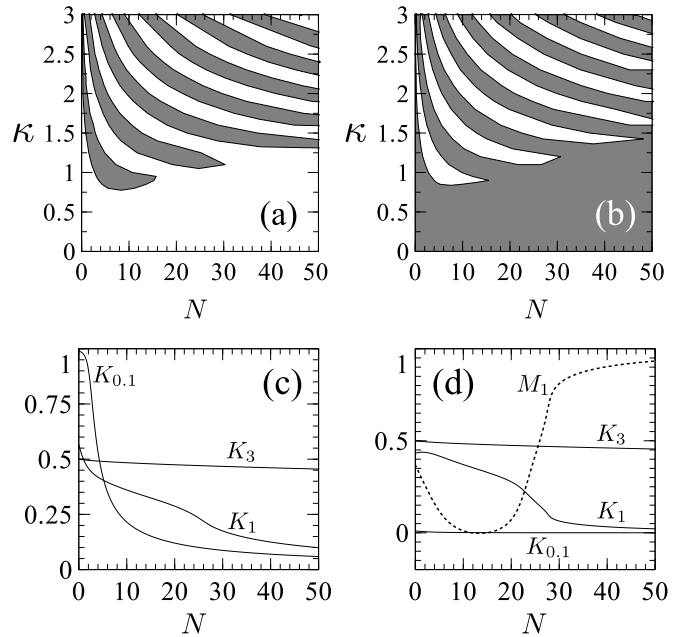


FIG. 4: (Color online) Stability domains (shaded) for odd (a) and even (b) nonlinear modes bifurcating from the lowest linear eigenstate, with $n = 0$, in the system with the SO coupling in the absence of the Zeeman splitting. (c) and (d): The overlap integral, K , versus the total norm, N , for odd (c) and even (d) modes. Curves labeled $K_{0,1,1,3}$ correspond to $\kappa = 0.1, 1$, and 3 , respectively. The dashed curve in (d) shows the total magnetic moment, M , as a function of N for $\kappa = 1$. For $\kappa = 0.1$ and $\kappa = 3$, M does not vary significantly with N . Other parameters are $g_1 = g/2 = 1$, $\Omega = 0$.

cibility factor,

$$K \equiv 4 \int_{-\infty}^{+\infty} |\phi_1|^2 |\phi_2|^2 dx \Big/ \int_{-\infty}^{+\infty} (|\phi_1|^2 + |\phi_2|^2)^2 dx, \quad (4)$$

which takes values $0 \leq K \leq 1$, with $K = 0$ and $K = 1$ corresponding, severally, to the completely immiscible or miscible state. Note that the immiscibility, $K \rightarrow 0$, may be achieved not only if the phases are spatially separated, but also if one phase disappears, and the condensate falls into a single-domain state, as in the case of the even mode in Fig. 1 (b). In the linear limit $N \rightarrow 0$, one has $\tilde{M} = e^{-\kappa^2}$ for the even eigenstates, and $\tilde{M} \equiv 0$ for the current and odd ones, while $\tilde{K} = (1 \mp e^{-2\kappa^2})/2$ for the odd ($-$) and even ($+$) states.

Figure 4(c) shows that the nonlinearity enhances the immiscibility of the odd modes, although the effect may be significantly reduced by the coupling, as curve K_3 demonstrates. The effect of the interplay between the nonlinearity and SO coupling is more sophisticated for even modes, see Fig. 4(d). When the SO coupling is sufficiently weak (curve $K_{0,1}$) or strong (curve K_3), the nonlinear modes preserve properties of their linear counterparts: at $\kappa = 0.1$ the mode is nearly fully polarized ($M_{0,1} \approx 1$, $K_{0,1} \ll 1$), while the mode with $\kappa = 3$ ($M_3 \ll 1$, $K_3 \approx 0.5$) represents a partially miscible state,

where both components are equally represented, with M close to zero.

The most interesting behavior is observed at intermediate values of the SO coupling, which corresponds to $\kappa = 1$ in panel (d). In this case, by changing norm N one draws the condensate into the immiscible state (curve K_1), and, at the same time, changes M between zero and its extreme value $+1$. Bearing in mind that the BEC nonlinearity may be controlled via the Feshbach resonance [27], the observed behavior suggests a possibility of switching between the different phases with the help of external fields.

IV. SYMMETRY BREAKING DUE TO THE ZEEMAN SPLITTING

In the linear limit $N \rightarrow 0$, the Zeeman splitting [$\Omega \neq 0$ in Eqs. (1)] removes the energy degeneracy. Now, the system does not admit current states and odd modes, while stable even modes, characterized by even $\phi_1(x)$ and odd $\phi_2(x)$ (or *vice versa*), persist at $\Omega \neq 0$. The evolution of the eigenstates under the action of the increasing Zeeman splitting, Ω , is illustrated by the bifurcation diagram in the plane of (M, Ω) , shown in Fig. 5. Starting with the point where an odd (even) mode is stable (unstable) at $\Omega = 0$, we observe a transformation of the stable odd mode into stable asymmetric ones [see an example in Fig. 5 (a)], whose branch approaches the branches of the even modes. The instability of the even modes persists up to the point where the branches of even and asymmetric modes merge (points $P_{1,2}$). At these points, the asymmetric modes disappear and the symmetric even ones become stable [an example is shown in Fig. 5(b)]. Thus, a pitchfork bifurcation occurs at points $P_{1,2}$, which is a typical example of the *spontaneous symmetry breaking* (or restoration) [33].

The bifurcation diagram in Fig. 5 suggests that, by varying the Zeeman field which induces the Zeeman splitting, one can perform a controllable switch between two opposite magnetizations in the SO-coupled binary system. This suggestion is confirmed by simulations, as shown in Fig. 6.

V. CONCLUSION

We have reported the existence of even, odd, and asymmetric nonlinear modes in the effectively 1D self-repulsive binary BEC with the SO and Zeeman splitting, confined by the axial HO potential. The interplay between the coupling and the potential gives rise to the modes featuring alternating domains with opposite directions of the pseudo-spin, which is explained analytically in the case of the weak nonlinearity. Noteworthy findings are the stability of the multi-DW patterns, while the one with the single DW is unstable, and the stability alternation between the even and odd structures. The implication

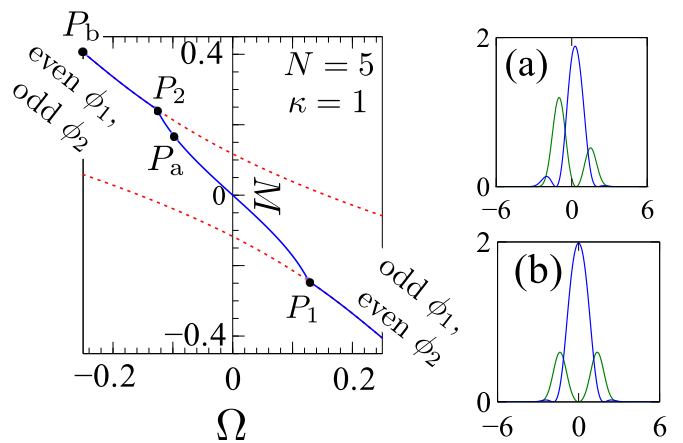


FIG. 5: (Color online) The bifurcation diagram (the left panel) for $\kappa = 1$ and $N = 5$, in the presence of the Zeeman splitting, Ω , the other parameters being as in Fig. 4. Stable (unstable) modes correspond to solid (broken) fragments of the curves. Panels (a) and (b) show profiles of stable modes marked by points $P_{a,b}$.

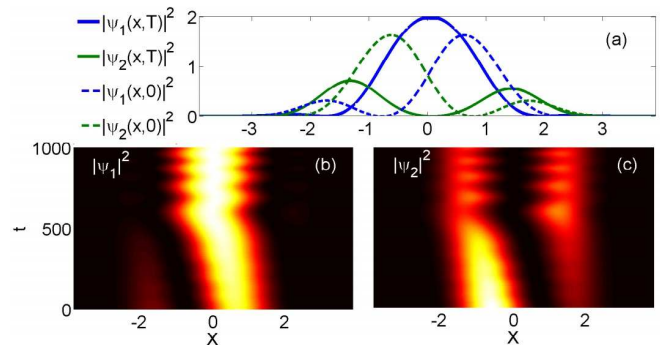


FIG. 6: (Color online) The evolution of a nonlinear mode subjected to an adiabatic change of Ω . Panel (a) shows the input and output spatial profiles. Panels (b) and (c) display intensity plots. The input at $t = 0$ is a stable odd mode at $\Omega = 0$, the other parameters being as in Fig. 5. In the course of the simulation, Ω was adiabatically changed from $\Omega = 0$ at $t = 0$ to $\Omega = -0.25$ at $t = 10^3$. As a result, the condensate switches from the initial odd mode to an even one, as predicted by the diagram in Fig. 5.

of these results is the transition from simple to complex ground states, driven by the SO coupling. The inclusion of the Zeeman splitting results in the transformation of even modes into asymmetric ones, which suggests a possibility of controllable switching between states with opposite pseudo-magnetization. These effects, including the transition to the complex ground states, may be as well expected in other physical setting emulated by the SO-coupled binary condensates, such as solid-state media and bimodal guided-wave propagation in optics.

VVK and DAZ acknowledge support of the FCT (Portugal) grants PEst-OE/FIS/UI0618/2011, and SFRH/BPD/64835/2009. The work of RD and BAM was supported, in a part by the Binational (US-Israel)

Science Foundation through grant No. 2010239.

-
- [1] P. Hauke, F. M. Cucchietti, L. Tagliacozzo, I. Deutsch, and M. Lewenstein, *Rep. Prog. Phys.* **75**, 082401 (2012).
- [2] Y. J. Lin, K. Jiménez-García, and I. B. Spielman, *Nature* **471**, 83 (2011).
- [3] J. Dalibard, F. Gerbier, G. Juzeliūnas, and P. Öhberg, *Rev. Mod. Phys.* **83**, 1523 (2011).
- [4] Y.-J. Lin, R. L. Compton, A. R. Perry, W. D. Phillips, J. V. Porto, and I. B. Spielman, *Phys. Rev. Lett.* **102**, 130401 (2009); Y.-J. Lin, R. L. Compton, K. Jiménez-García, J. V. Porto, and I. B. Spielman, *Nature (London)* **462**, 628 (2009).
- [5] T.-L. Ho and S. Zhang, *Phys. Rev. Lett.* **107**, 150403 (2011).
- [6] X.-Q. Xu and J. H. Han, *Phys. Rev. Lett.* **107**, 200401 (2011); J. Radić, T. A. Sedrakyan, I. B. Spielman, and V. Galitski, *Phys. Rev. A* **84**, 063604 (2011); B. Ramachandhran, B. Opanchuk, X.-J. Liu, H. Pu, P. D. Drummond, and H. Hu, *ibid.* **85**, 023606 (2012); H. Sakaguchi and B. Li, *ibid.* **87**, 015602 (2013); X.-F. Zhou, J. Zhou, and C. Wu, *Phys. Rev. A* **84**, 063624 (2011).
- [7] G. J. Conduit, *Phys. Rev. A* **86**, 021605(R) (2012).
- [8] C. Wang, C., Gao, C.-M. Jian, and H. Zhai, *Phys. Rev. Lett.* **105**, 160403 (2010).
- [9] S. Sinha, R. Nath, and L. Santos, *Phys. Rev. Lett.* **107**, 270401 (2011).
- [10] Y. Li, L. P. Pitaevskii, and S. Stringari, *Phys. Rev. Lett.* **108**, 225301 (2012).
- [11] T. Kawakami, T. Mizushima, M. Nitta, and K. Machida, *Phys. Rev. Lett.* **109**, 015301 (2012); Y. Li, X. Zhou, and C. Wu, arXiv:1205.2162.
- [12] V. Achilleos, D. J. Frantzeskakis, P. G. Kevrekidis, and D. E. Pelinovsky, arXiv:1211.0199.
- [13] Y. Xu, Y. Zhang, and B. Wu, *Phys. Rev. A* **87**, 013614 (2013).
- [14] W. Han, S. Zhang, and W.-M. Liu, arXiv:1211.2097v3 (2013).
- [15] B. A. Malomed, *Phys. Rev. A* **43**, 410 (1991).
- [16] R. Keil, J. M. Zeuner, F. Dreisow, M. Heinrich, A. Tünemann, S. Nolte, and A. Szameit, *Nat. Commun.* **4**, 1368 (2013).
- [17] Y. Zhang, Li Mao, and C. Zhang, *Phys. Rev. Lett.* **108**, 035302 (2012).
- [18] Y. V. Kartashov, V. A. Vysloukh, L. Torner, and B. A. Malomed, *Opt. Lett.* **36**, 4587 (2011).
- [19] Y. A. Bychkov and E. I. Rashba, *J. Phys. C* **17**, 6039 (1984).
- [20] G. Dresselhaus, *Phys. Rev.* **100**, 580 (1955).
- [21] M. J. Edmonds, J. Otterbach, R. G. Unanyan, M. Fleischhauer, M Titov, and P. Öhberg, *New J. Phys.* **14**, 073056 (2012).
- [22] L. Salasnich, A. Parola, and L. Reatto, *Phys. Rev. A* **65**, 043614 (2002); A. E. Muryshev, G. V. Shlyapnikov, W. Ertmer, K. Sengstock, and M. Lewenstein, *Phys. Rev. Lett.* **89**, 110401 (2002); Y. B. Band, I. Towers, and B. A. Malomed, *Phys. Rev. A* **67**, 023602 (2003); V. A. Brazhnyi and V. V. Konotop, *ibid.* **68**, 43613 (2003); L. D. Carr and J. Brand, *Phys. Rev. Lett.* **92**, 040401 (2004); A. Muñoz Mateo and V. Delgado, *Phys. Rev. A* **75**, 063610 (2007); **77**, 013617 (2008).
- [23] L. Salasnich and B. A. Malomed, *Phys. Rev. A* **74**, 053610 (2006).
- [24] L. Salasnich and B. A. Malomed, *Phys. Rev. A* **87**, 063625 (2013).
- [25] The inner product used here is defined as $\langle \mathbf{a}, \mathbf{b} \rangle = \int_{-\infty}^{+\infty} [a_1^*(x)b_1(x) + a_2^*(x)b_2(x)] dx$.
- [26] V. P. Mineev, *Zh. Eksp. Teor. Fiz.* **67**, 263 (1974) [*Sov. Phys. JETP* **40**, 132 (1974)].
- [27] C. Pethick and H. Smith, *Bose-Einstein Condensation in Dilute Gases* (Cambridge University Press: Cambridge, 2002); L. P. Pitaevskii and S. Stringari, *Bose-Einstein Condensation* (Clarendon Press: Oxford and New York, 2003).
- [28] M. I. Merhasin, B. A. Malomed, and R. Driben, *J. Phys. B: At. Mol. Opt. Phys.* **38**, 877 (2005).
- [29] M. Trippenbach, K. Góral, K. Rzazewski, B. Malomed, and Y. B. Band, *J. Phys. B: At. Mol. Opt.* **33**, 4017 (2000); K. Kasamatsu, Y. Yasui, and M. Tsubota, *Phys. Rev. A* **64**, 053605 (2001); K. Kasamatsu, M. Tsubota, and M. Ueda, *Int. J. Mod Phys B* **19**, 1835 (2005).
- [30] M. Matuszewski, T. J. Alexander, and Yu. S. Kivshar, *Low Temp. Phys.* **36**, 700 (2010).
- [31] Z. F. Xu, R. Lü, and L. You, *Phys. Rev. A* **83**, 053602 (2011).
- [32] T. Ozawa, L. P. Pitaevskii, S. Stringari, arXiv:1305.0645.
- [33] B. A. Malomed (editor), *Spontaneous Symmetry Breaking, Self-trapping, and Josephson Oscillations* (Springer, 2013).